Isothianaphthene-Based Conjugated Polymers for Organic Photovoltaic Cells

Guankui Long, Xiangjian Wan,* Jiaoyan Zhou, Yongsheng Liu, Zhi Li, Guangrui He, Mingtao Zhang, Yanhui Hou, Yongsheng Chen*

Two novel copolymers PBDT-DEAITN and PBDT-DOAITN containing the same backbone of isothianaphthene (ITN) quinoidal and benzodithiophene (BDT) donor units are synthesized and their organic photovoltaic (OPV) devices are fabricated. Although these two polymers have rather low optical bandgaps, 1.52 and 1.58 eV for PBDT-DEAITN and PBDT-DOAITN, respectively, their OPV cells exhibit rather limited power conversion efficiencies of 1.25% and 1.20% under an AM1.5G simulated solar light. The reasons for the low OPV performance are investigated by structure modeling calculation. Based on this and the screening results for the representative quinoidal polymers in the literatures, a strategy of designing high-performance planar polymers based on ITN unit is proposed.

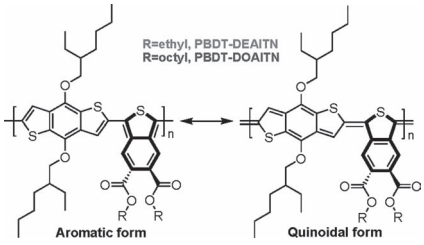

1. Introduction

Solution-processed organic photovoltaic (OPV) cells have drawn tremendous interest in the past decade, for the prospect of a renewable energy source due to their eminent advantages such as light weight, high material utilization, solution process (roll to roll, spin coating), low cost, and high mechanical flexibility.[1–3] The performance of OPV has increased dramatically recently and power conversion efficiency (PCE) up to 7% has been achieved by using low-bandgap polymers in the bulk heterojunction (BHJ) structure solar cells.[4–17] Two different strategies are usually employed in developing new low-bandgap polymers. The first and most common one is the donor-acceptor (D-A) approach through intramolecular charge transfer,[18–20] the second and much less explored approach to obtain low bandgap is through the quinoidal resonance structure stabilization.[21–23] Representative quinoidal units with its aromatic form were presented in Figure 1.

Recently, Yu and co-workers[21,24] have developed a series of new semiconducting polymers with thieno[3,4-b]thiophene (TT) and benzodithiophene (BDT) alternating units, with PCE over 8%.[4] These TT-based polymers can support the quinoidal structure and lead to a narrow polymer bandgap, which is crucial to efficiently harvest solar energy.

Thieno[3,4-b]pyrazine (TP) is another quinoidal building block,[25] which would reduce the significant steric interactions between the pyrazine nitrogen and neighboring thiophene thus facilitates to get planar backbone geometry.[26] TPs have been shown to be very successful in producing low-bandgap conjugated materials. However, the best devices for TP-based materials to date utilizing the arylalkyne copolymer gave only a moderate PCE of 2.37%.[27] Partial reason for this could be that most of the reported TP materials have low molecular weight due to the limits of solubility for the introduction of nitrogen atoms, and the lowest unoccupied molecular orbital (LUMO) of these materials is difficult to tune for their intrinsic strong electron-deficient nature of the TP block.[25]

G. Long, X. Wan, J. Zhou, Y. Liu, Z. Li, G. He, Y. Chen
Key Laboratory for Functional Polymer Materials and Center for Nanoscale Science and Technology, Institute of Polymer Chemistry, College of Chemistry, Nankai University, Tianjin 300071, P. R. China
E-mail: xjwan@nankai.edu.cn; yscheng99@nankai.edu.cn
M. Zhang
Computational Center for Molecular Science, College of Chemistry, Nankai University, Tianjin 300071, P. R. China
Y. Hou
School of Materials Science and Engineering, Tianjin Key Laboratory of Fiber Modification and Functional Fiber, Tianjin Polytechnic University, Tianjin 300160, P. R. China

DOI: 10.1002/macp.201200142

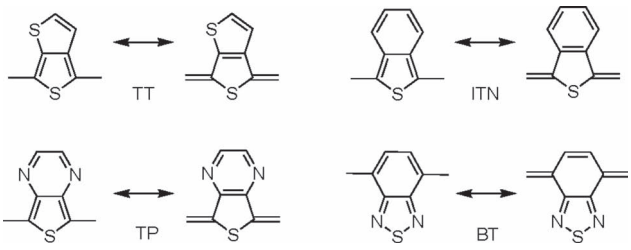

Figure 1. Aromatic and quinoidal form of thieno[3,4-b]thiophene (TT), isothianaphthene (ITN), thienopyrazine(TP), and benzothiadiazole (BT) units.

Benzothiadiazole (BT) is one of the most widely used quinoidal acceptor units in low-bandgap polymers, which is the isoelectronic species of TP. The lone pair of nitrogen atom in BT would interact with the hydrogen atom in adjacent unit thus could minimize the steric hindrance.[28] The most famous **PCDTBT** (poly[[9-(1-octylnonyl)-9H-carbazole-2,7-diyl]-2,5-thiophenediyl-2,1,3-benzothiadiazole-4,7-diyl-2,5-thiophenediyl]) and **PSBTBT** (poly[(4,4'-bis-(2-ethylhexyl)dithieno[3,2-b:2',3'-d]silole)-2,6-diyl-alt-(2,1,3-benzothiadiazole-4,7-diyl]) have reached PCE of 7.2%[16,17] and 5.9%.[29]

Another important quinoidal unit is isothianaphthene (ITN, or benzo[c]thiophene),[30] which was proved to have higher quinoidal resonance energy than TT.[31] However, this unit is proved to be very unstable. Although much effort has been carried to use this block in low-bandgap polymers, only a few of examples were successful. Hillmyer and co-workers[32,33] had synthesized three types ITN-containing copolymer with fluorene (**PITN-*co*-FI**), thiophene (**PITN-*co*-3HT** and **PITN-*co*-3DT**), and BT (**PITN-*co*-ThBTD**). However, these polymers have low molecular weight and poor absorption in the visible region, except that polymer **PITN-*co*-ThBTD** exhibits a large red shift from solution to film with edge to 800 nm. OPV devices based on this polymer with $PC_{61}BM$ (1:4, w:w) exhibited only a PCE of 0.9%, which is the highest PCE for ITN-based polymers.[33] The low PCE and poor absorption of **PITN-*co*-FI** were ascribed to the large dihedral angle between two adjacent units (40.50 based on our calculation results), electron-rich nature of ITN and low molecular weight.

The non-planar structure,[26,34] low molecular weight,[35–40] and poorer film quality[41] therefore low crystallinity perhaps are the critical reasons for the poor OPV performance of ITN-based materials today. Inspired by Yu's pioneer work, herein, we introduced two electron-withdrawing ester groups onto ITN, expecting to stabilize the quinoidal unit for solving the synthesis issues and obtain high polymerization degree products with good solubility and thus achieve good film qualities during the device fabrication process. The initial results confirmed our design, OPV devices based on **PBDT-DEAITN** and **PBDT-DOAITN** as donors and $PC_{61}BM$ as the acceptor exhibit PCE around 1.2% under an AM1.5G simulated solar light at 100 mW cm^2, which is the best results for ITN-based OPV devices. The reasons behind the low PCEs, compared with other polymers, of these two polymers are investigated and the large dihedral angles between BDT and ITN units in the polymers are believed to be one of the major causes.

2. Experimental Section

2.1. Instruments

The ^1H NMR spectra were recorded on a Bruker AV400 Spectrometer. Gel permeation chromatography (GPC) analysis was conducted on a Waters 510 system using polystyrene as the standard and tetrahydrofuran (THF) as the eluent at a flow rate of 1.0 mL min^{-1} at 40 °C. Thermal gravimetric analysis (TGA) was performed on a NETZSCH STA 409PC instrument under purified nitrogen gas flow with a 10 °C min^{-1} heating rate. The temperature of degradation (T_d) corresponds to a 5% weight loss. X-ray diffraction (XRD) experiments were performed on a Rigaku D/max-2500 X-ray diffractometer with Cu-K_α radiation (k = 1.5406) at a generator voltage of 40 kV and a current of 100 mA. Atomic force microscope (AFM) was performed using SII SPA-400 AFM in tapping mode. The UV-Vis spectra were obtained with a JASCO V-570 spectrophotometer. Cyclic voltammetry (CV) experiments were performed with an LK98B II microcomputer-based electrochemical analyzer. All measurements were carried out at room temperature with a conventional three-electrode configuration employing a glassy carbon electrode as the working electrode, a saturated calomel electrode (SCE) as the reference electrode, and a Pt wire as the counter electrode. CH_3CN was distilled over calcium hydride under dry argon immediately prior to use. Tetrabutylammonium hexafluorophosphate (Bu_4NPF_6, 0.1 M) in CH_3CN was used as the supporting electrolyte, and the scan rate was 100 mV s^{-1}, highest occupied molecular orbital (HOMO) and LUMO levels were estimated relative to the energy level of a ferrocene reference (4.8 eV below vacuum level).

2.2. Materials

All reactions and manipulations were carried out under argon atmosphere with the use of standard Schlenk techniques. All starting materials were purchased from commercial suppliers and used without further purification. 2,6-Bis(trimethyltin)-4,8-bis(2-ethylhexyloxy)benzo[1,2-b:4,5-b]dithiophene (**1**),[42] diethyl 1,3-dibromobenzo[c]thiophene-5,6-dicarboxylate (**2**), and dioctyl 1,3-dibromobenzo[c]thiophene-5,6-dicarboxylate (**3**)[43,44] were prepared according to the reported methods. As shown in Scheme 1, the low-bandgap polymers **PBDT-DEAITN** and **PBDT-DOAITN** were synthesized by Stille coupling polymerization of the monomers of **2** or **3** with **1** using tris(dibenzylideneacetone) dipalladium[0] ($Pd_2(dba)_3$) and tri(o-tolyl)phosphine ($P(o\text{-}tolyl)_3$) as the catalyst in yields around 90%.

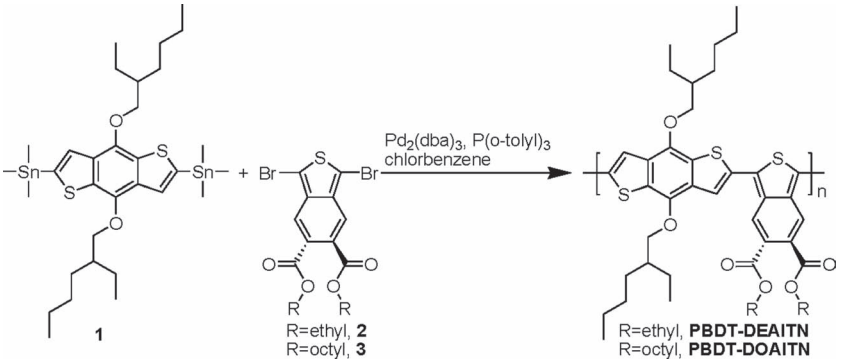

Scheme 1. Synthesis of polymers via palladium-catalyzedcouplingreactions.

2.3. Polymer Synthesis

2.3.1. PBDT-DEAITN

Diethyl 1,3-dibromobenzo[c]thiophene-5,6-dicarboxylate (350 mg, 0.80 mmol), 2,6-bis(trimethyltin)-4,8-bis(2-ethylhexyloxy) benzo[1,2-b:4,5-b]dithiophene (621 mg, 0.80 mmol), and P(o-tolyl)$_3$ (26.3 mg, 0.064 mmol) were dissolved in 10 mL dry chlorobenzene. The mixture was purged by argon, then bubbled with argon for 20 min, $Pd_2(dba)_3$ (15 mg, 0.016 mmol) was added. After being purged with argon, the mixture was refluxed at 110 °C for 24 h. After cooling to room temperature, the organic solution was added dropwise to 250 mL methanol to obtain precipitate, which was collected by filtration and washed with methanol and dried. Then the precipitate was subjected to Soxhlet extraction with methanol, hexane, and chloroform, respectively. The chloroform fraction was concentrated and obtained by precipitation from methanol. Then the residue was dried under vacuum and affording a black solid powder. Yield: 523.4 mg, 90.3%, $\overline{M}_n$ = 27.54 kDa, PDI = 2.14; ^{1}H NMR (400M, $CDCl_3$, δ): 8.56 (m, 1H), 8.29 (m, 1H), 7.82 (m, 1H), 7.48 (m, 1H), 4.44 (br, 4H), 4.31 (br, 4H), 1.91–1.46 (m, 24H), 1.10 (m, 12H) ppm.

2.3.2. PBDT-DOAITN

The synthesis procedure was similar with that of **PBDT-DEAITN** except replacement of monomer diethyl 1,3-dibromobenzo[c] thiophene-5,6-dicarboxylate (**2**) with dioctyl 1,3-dibromobenzo[c] thiophene-5,6-dicarboxylate (**3**). The polymer was obtained with yield of 90.9%, $\overline{M}_n$ = 16.74 KDa, PDI = 2.38; ^{1}H NMR (400M, $CDCl_3$, δ): 8.57 (m, 1H), 8.35 (m, 1H), 7.82 (m, 1H), 7.71 (m, 1H), 4.30 (br, 8H), 1.92–1.26 (m, 36H), 1.10–0.80 (m, 24H) ppm.

2.4. Polymer Solar Cell Fabrication and Testing

All the photovoltaic devices were fabricated by using a common solution process. An ITO-coated glass substrate was cleaned stepwise in detergent, distilled water, acetone, and isopropyl alcohol under ultrasonication for 15 min each and subsequently dried by a nitrogen blow. A thin layer of PEDOT:PSS (Baytron P VP AI 4083, filtered at 0.45 μm) was spin-coated (4000 rpm, ca. 40 nm thick) onto ITO surface. After being baked at 150 °C for 20 min, the substrates were transferred into an argon-filled glove box. Subsequently, the active layer was spin-coated from different blend ratios (weight-to-weight) of donor and $PC_{61}BM$ in *o*-dichlorobenzene (ODCB) solution at 1500 rpm for 60 s on the ITO/PEDOT:PSS substrate without further special treatments. The active layer thickness was measured as ca. 80 nm using a Dektak 150 profilometer. Finally, 1 nm LiF layer and 80 nm Al layer were deposited on the active layer under high vacuum (<3 × 10^{-4} Pa). The effective area of each cell was 4 mm^2 defined by masks for all the solar cell devices discussed in this work.

2.5. Hole Mobility

Hole mobility was measured using a diode configuration of ITO/PEDOT:PSS/Polymer/Al by taking dark current in the range of 0–6 V and fitting the results to a space charge limited form, where the space charge limited current (SCLC) is described by:

$$J^{\frac{1}{2}} = \left(\frac{9\varepsilon_0\varepsilon_r\mu_h}{8L^3}\right)^{\frac{1}{2}}\left(V_{appl} - V_{bi} - V_r\right) = kV_{appl} - kC$$

$$k = \left(\frac{9\varepsilon_0\varepsilon_r\mu_h}{8L^3}\right)^{\frac{1}{2}};\ C = V_{bi} + V_r$$

where J is the current density, L is the film thickness of the active layer, μ_h is the hole mobility, ε_r is the relative dielectric constant of the transport medium, ε_0 is the permittivity of free space, V is the internal voltage in the device, and $V = V_{appl} - V_{bi} - V_r$, where V_{appl} is the applied voltage to the device, V_r is the voltage drop as a result of contact resistance and series resistance across the electrodes, and V_{bi} is the built-in voltage attributed to the relative work function difference of the two electrodes.

3. Results and Discussion

3.1. Polymer Synthesis and Characterization

The synthesis is outlined in Scheme 1, both **PBDT-DEAITN** and **PBDT-DOAITN** have readily good solubility in common organic solvents such as chloroform, chlorobenzene, and ODCB owing to the existence of four alkyl chains in each repeat unit. As shown in Table 1, the number-averaged molecular weight ($\overline{M}_n$) and polydispersity (PDI) were

Table 1. Polymerization results for **PBDT-DEAITN** and **PBDT-DOAITN.**

Polymer	Yield [%]	$\overline{M}_n$ [Kg mol^{-1}]$^{a)}$	$\overline{M}_w$ [Kg mol^{-1}]$^{a)}$	PDI	T_d [°C]$^{b)}$
PBDT-DEAITN	90.3	27.54	58.92	2.14	333
PBDT-DOAITN	90.9	16.74	39.89	2.38	335

$^{a)}$Determined by GPC in THF using polystyrene standards; $^{b)}$The temperature of degradation corresponding to a 5% weight loss determined by TGA at a heating rate of 10 °C min^{-1}.

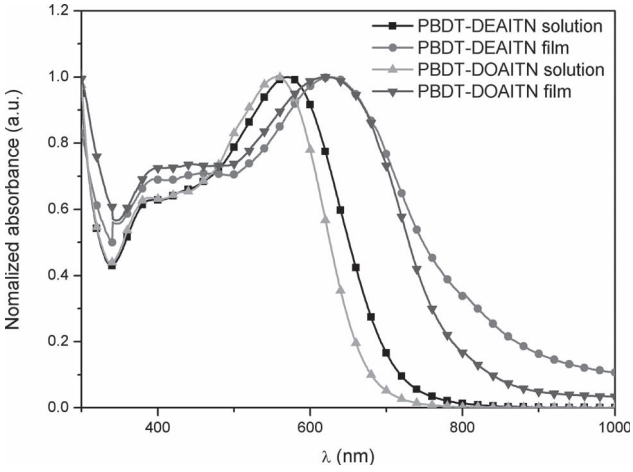

Figure 2. UV–Vis spectra of all polymers: **PBDT-DEAITN**, **PBDT-DOAITN** in chloroform and in solid film.

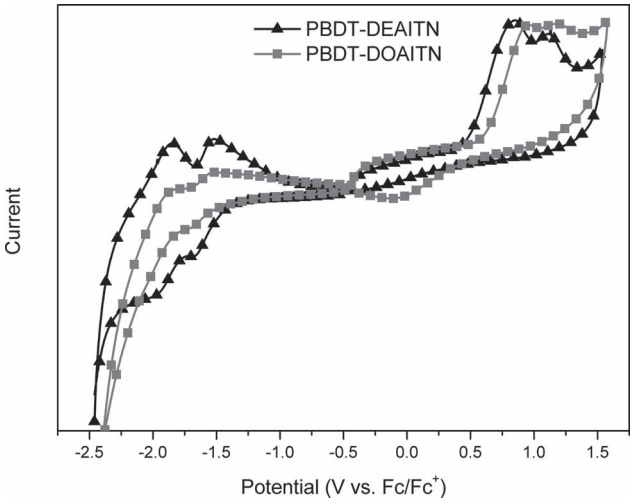

Figure 3. Cyclic voltammograms of the oxidation and reduction behavior of thin films of **PBDT-DEAITN** and **PBDT-DOAITN**.

$\overline{M}_n$ = 27.54 kDa, PDI = 2.14 for **PBDT-DEAITN** and $\overline{M}_n$ = 16.74 kDa, PDI = 2.38 for **PBDT-DOAITN** using GPC calibrated relative to polystyrene standards. In most cases, the molecular weight of ITN-based polymer was lower than 10 kDa,[32,33,45] Hillmyer and co-workers[32] had pointed out that the low molecular weight probably owing to the electron-rich nature of ITN may slow down the insertion and destabilize the complex leading to side reactions and possible deactivation of the catalyst of Pd[0]-catalyzed coupling reaction. TGA suggests that both polymers exhibit good stability with a T_d greater than 330 °C under a N_2 atmosphere (as shown in Table 1).

3.2. Optical and Electrochemical Properties

The absorption spectra of **PBDT-DEAITN** and **PBDT-DOAITN** in dilute chloroform solution and in the solid state were shown in Figure 2 and summarized in Table 2. Both **PBDT-DEAITN** and **PBDT-DOAITN** exhibited two bands in the solution and solid state. The peaks at the shorter wavelength corresponding to the π–π* absorption of the two polymers nearly have no difference with maximum absorption peaks at 389 nm for solution and 403 nm for the solid. While **PBDT-DEAITN** showed less red shift compared with **PBDT-DOAITN** in both solution and film state at longer wavelength. Both polymers showed about 60 nm red-shift from solution to film, which were 56 nm (from 570 to 626 nm) for **PBDT-DEAITN** and 65 nm (from 557 to 622 nm) for **PBDT-DOAITN**. The optical bandgap of **PBDT-DEAITN** and **PBDT-DOAITN** in film state is comparable, which was estimated to be 1.52 and 1.58 eV by extrapolation of the low-energy edge of the absorption spectra.

Cyclic voltammograms (CVs) were recorded from thin films of **PBDT-DEAITN** and **PBDT-DOAITN** drop-casted from chloroform solutions as described in the Section 2.[46] Figure 3 displays the CV curves for these two polymers, and the potentials were internally calibrated using the ferrocene/ferrocenium (Fc/Fc^+) redox couple (4.8 eV below the vacuum level). From the onset oxidation potentials (E_{ox}) and the onset reduction potentials (E_{red}) of the polymers, HOMO and LUMO energy levels of the polymers were calculated according to the equations: HOMO = $-e(E_{ox} + 4.8)$ (eV) and LUMO = $-e(E_{red} + 4.8)$ (eV). The results of the electrochemical measurements are listed in Table 2, these two polymers exhibit deeper HOMO energy levels compared with reported ITN analogues,[35,39,45] which are beneficial to achieve high V_{oc}. The HOMO level of **PBDT-DOAITN** (–5.42 eV) is 0.12 eV lower than that of **PBDT-DEAITN** (–5.30 eV), probably due to longer alkyl side chains, which would weaken the π-overlapping among individual conjugated polymer chains and therefore result in weaker intermolecular interaction.[47,48] Based on the calculation structures of **PBDT-DEAITN** and **PBDT-DOAITN** discussed below, the two alkyl groups of ITN units tend to minimize the steric hindrance through arranging the two alkyl groups onto the different side of ITN plane (as shown in Scheme 1). The electrochemical bandgap of both polymers is somewhat larger than its optical bandgap, similar phenomena have been observed in the studies of other D-A

Table 2. Optical and electrochemical data of **PBDT-DEAITN** and **PBDT-DOAITN**.

	UV –Visabsorption				Cyclic voltammetry		
	λ_{max} [nm]	λ_{max} [nm]	λ_{onset} [nm]	E_g [eV]	HOMO [eV]	LUMO [eV]	E_g [eV]
PBDT-DEAITN	570	626	814	1.52	–5.30	–3.38	1.92
PBDT-DOAITN	557	622	784	1.58	–5.42	–3.33	2.09

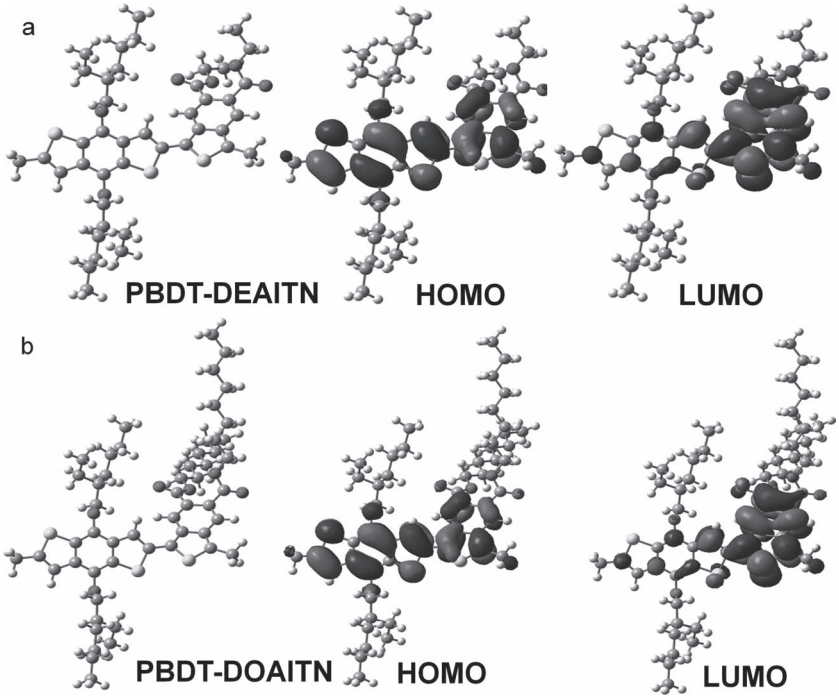

Figure 4. Optimized geomery and HOMO, LUMO electron-density distributions of **PBDT-DEAITN** (a) and **PBDT-DOAITN** (b).

polymers,[42,49–51] presumably resulting from the interface barrier for charge injection.[42,52]

3.3. Computational Study

Computational studies were employed to investigate the intrinsic properties and differences of **PBDT-DEAITN**, **PBDT-DOAITN,** and other representative quinoidal polymers (structures were shown in Figure S8, Supporting Information). To simplify the calculation, only one repeating unit of each polymer was subject to the calculation. All of the density functional theory calculations without special mentioned were performed with the Gaussian 09 program package[53] with the B3LYP function[54,55] and a 6-31g(d) basis set, and the frequency analysis was followed to assure that the optimized structures were stable states. The optimized geometry and simulated electron-density distributions were shown in Figure 4 and Supporting Information, and the calculated HOMO and LUMO levels are listed in Table 3. Compared with **PBDT-ITN**, **PBDT-DEAITN,** and **PBDT-DOAITN,** which have electron-withdrawing groups onto the ITN unit, the calculated HOMO levels of **PBDT-ITN** shifts from –4.84 to –5.03 eV, therefore increase the stability of ITN-based materials. As shown in Figure 4, for **PBDT-DEAITN** and **PBDT-DOAITN**, the electron density of LUMO is more localized on the ITN unit, which means that the introduction of electron-withdrawing groups onto ITN units has changed their electron-rich nature to electron-deficient. Meanwhile, the electron density of HOMO of these two polymers is delocalized over the whole conjugated backbone, and different alkyl groups have little effect on the electron-density distribution of frontier molecular orbital. The dihedral angles between BDT and ITN units for **PBDT-DEAITN** and **PBDT-DOAITN** were 33.66° and 34.35°, which is obviously larger than other quinoidal-based polymers (19.01° for **PBDTTT-CF**, and only 0.82° for **PBDT-TP**[42]). The significantly larger dihedral angle of **PBDT-DEAITN** and **PBDT-DOAITN** is owing to the repulsion between sulfur atom (BDT) and hydrogen atom on the phenyl ring (ITN),[26,34] and this causes the polymer packing less ordered in solid state with low hole mobility, thus poor OPV performance. Recent experiment and theoretical results showed that large local dipole moment existing in one of the monomer units in the donor polymers plays an important role in charge separation and carrier generation, thus would be facilitate to obtain high PCE.[56,57] As shown in Table 3, among all these polymers, **PBDTTT-CF** has the largest dipole moment and hole mobility, therefore the best OPV performance.

3.4. Photovoltaic Properties

The photovoltaic properties of **PBDT-DEAITN** and **PBDT-DOAITN** were explored based on BHJ devices with the standard sandwich structure ITO/PEDOT:PSS(40 nm)/polymer:$PC_{61}BM$/LiF(1 nm)/Al(80 nm) using the simple solution process from their ODCB solutions. All OPV

Table 3. Calculated results and measured mobility of representative quinoidal polymers.

	Dihedral [°]	Dipole [D]	HOMO [eV]	LUMO [eV]	Mobility [$cm^2\ V^{-1}\ s^{-1}$][a)]
PBDT-DEAITN	33.66	0.81	–5.04	–2.15	2.36×10^{-5}
PBDT-DOAITN	34.35	0.50	–5.03	–2.13	2.86×10^{-5}
PBDT-ITN	35.89	0.45	–4.84	–1.74	None
PBDT-TP	0.82	0.03	–4.92	–2.43	None
PBDTTT-CF	19.01	3.11	–5.06	–2.09	7×10^{-4}

[a)]The mobilities were from SCLC results.[6]

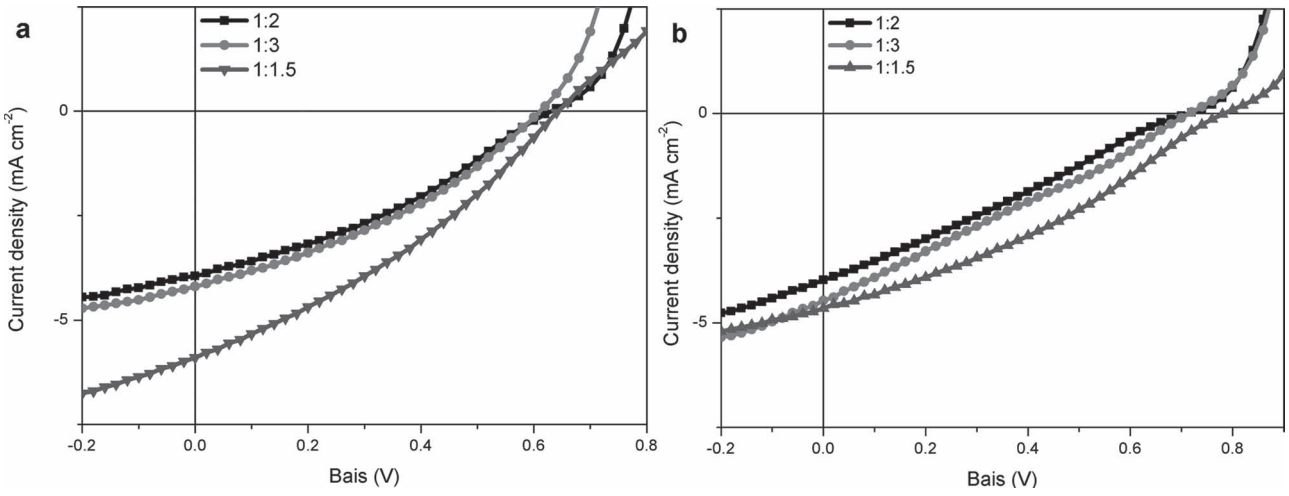

Figure 5. Characteristic J–V curves of the optimized devices of **PBDT-DEAITN** (a) and **PBDT-DOAITN** (b) with different ratios-based BHJ solar cells under simulated AM1.5G illumination (100 mW cm^{-2}).

devices were tested under simulated AM1.5G illumination (100 mW cm^{-2}). Device optimizations were conducted by varying ratios of polymer versus $PC_{61}BM$, and film thicknesses. Typical current density-voltage (J–V) characteristics were shown in Figure 5 and summarized in Table 4. The optimized PCEs were 1.25% and 1.20% for **PBDT-DEAITN** and **PBDT-DOAITN**, respectively. Both polymers showed very low fill factor (*FF*) around 0.30, probably due to the low charge mobility. The hole mobility for **PBDT-DEAITN** and **PBDT-DOAITN** was 2.36×10^{-5} and 2.86×10^{-5} cm^2 V^{-1} s^{-1} based on SCLC results.[58,59] Both **PBDT-DEAITN** and **PBDT-DOAITN** films showed no clear peak in their XRD analysis (Figure S4, Supporting Information) and thus they exist as amorphous material in solid state. This is probably owing to the large dihedral between the adjacent units as calculated above, which is consistent with the measured low mobility. OPV devices based on **PBDT-DOAITN** showed larger V_{oc} than **PBDT-DEAITN**, which is in agreement with the CV data. Recent theoretical and experiment results showed that reducing the electronic coupling between the donors and acceptors will suppress the charge-transfer band oscillator strength and reduce dark saturation current, and thus increase V_{oc}.[60,61] Therefore, longer side chains such as the two octyl chains of **PBDT-DOAITN** would weaken the intermolecular interaction, which is beneficial to get higher V_{oc} for **PBDT-DOAITN** than **PBDT-DEAITN**.[48]

In order to understand the effect of morphology of the active layers on their OPV device performance of these polymers, the surface morphology of blend film (w:w, 1:1.5) of **PBDT-DEAITN** or **PBDT-DOAITN** with $PC_{61}BM$ spin-coated from ODCB solutions was studied by tapping-mode AFM, and the topography and phase images are shown in Figure S2 (Supporting Information). The root mean square (rms) roughness of blend films is 0.58 nm for **PBDT-DEAITN**/$PC_{61}BM$ and 0.36 nm for **PBDT-DOAITN**/$PC_{61}BM$ with the blend ratio of 1:1.5, indicating different miscibility between the copolymers and $PC_{61}BM$. In consistent with the XRD data above, the films of these two polymers did not show clear crystalline morphology from AFM images. This is in contrast to P3HT[62,63] and other low-bandgap polymers with excellent charge mobilities.[5,11,24,64–66] All these probably contributed to the low hole mobilities, short circuit currents (J_{sc}) and thus poor OPV performance for **PBDT-DEAITN** and **PBDT-DOAITN**.

Table 4. OPV performances of PBDT-DEAITN and PBDT-DOAITN.

Polymer	Polymer:$PC_{61}BM$	V_{oc} [V]	J_{sc} [mA cm^{-2}]	*FF*	PCE [%]
PBDT-DEAITN	1:2	0.64	3.94	0.33	0.83
PBDT-DEAITN	1:3	0.62	4.19	0.34	0.88
PBDT-DEAITN	1:1.5	0.64	5.90	0.33	1.25
PBDT-DOAITN	1:2	0.72	3.97	0.26	0.74
PBDT-DOAITN	1:3	0.72	4.46	0.26	0.83
PBDT-DOAITN	1:1.5	0.78	4.65	0.33	1.20

4. Conclusion

In summary, two quinoidal copolymers **PBDT-DEAITN** and **PBDT-DOAITN** were successfully synthesized with high yields and characterized, these two polymers exhibited rather low optical bandgaps, number-averaged molecular weight

more than 10 kDa and better film quality compared with other ITN-based polymers reported in literatures. Polymer solar cells based on these two polymers as donors and $PC_{61}BM$ as the acceptor exhibit PCEs around 1.2%, which is the best performance for ITN-based OPV devices. The differences among the representative quinoidal polymers were discussed on the basis of theoretical calculations, which demonstrates that small dihedral angle between the adjacent units would result in a planar conjugated backbone, leading to low bandgap and high mobility, therefore better PCE. Future work should be focus on synthesizing planar polymers based on ITN units.

Supporting Information

Supporting Information is available from the Wiley Online Library or from the author

Acknowledgements: This work was supported by MOST (Grants 2012CB933401 and 2011DFB50300) and NSFC (Grants 50933003, 50902073, 50903044, and 21004043), and NSF of Tianjin City (Grant 10ZCGHHZ00600).

Received: March 20, 2012; Revised: May 3, 2012; Published online: July 3, 2012; DOI: 10.1002/macp.201200142

Keywords: DFT calculations; dihedral; isothianaphthene; organic photovoltaics; quinoidal polymers

[1] Y. J. Cheng, S. H. Yang, C. S. Hsu, *Chem. Rev.* **2009**, *109*, 5868.
[2] P. M. Beaujuge, J. M. Frechet, *J. Am. Chem. Soc.* **2011**, *133*, 20009.
[3] E. Bundgaard, F. C. Krebs, *Sol. Energy Mater. Sol. Cell* **2007**, *91*, 954.
[4] Z. He, C. Zhong, X. Huang, W. Y. Wong, H. Wu, L. Chen, S. Su, Y. Cao, *Adv. Mater.* **2011**, *23*, 4636.
[5] Y. Liang, Z. Xu, J. Xia, S. T. Tsai, Y. Wu, G. Li, C. Ray, L. Yu, *Adv. Mater.* **2010**, *22*, E135.
[6] H. Y. Chen, J. Hou, S. Zhang, Y. Liang, G. Yang, Y. Yang, L. Yu, Y. Wu, G. Li, *Nat. Photon.* **2009**, *3*, 649.
[7] S. C. Price, A. C. Stuart, L. Q. Yang, H. X. Zhou, W. You, *J. Am. Chem. Soc.* **2011**, *133*, 4625.
[8] H. X. Zhou, L. Q. Yang, A. C. Stuart, S. C. Price, S. B. Liu, W. You, *Angew. Chem.Int. Ed.* **2011**, *50*, 2995.
[9] C. E. Small, S. Chen, J. Subbiah, C. M. Amb, S. W. Tsang, T. H. Lai, J. R. Reynolds, F. So, *Nat. Photon.* **2012**, *6*, 115.
[10] C. M. Amb, S. Chen, K. R. Graham, J. Subbiah, C. E. Small, F. So, J. R. Reynolds, *J. Am. Chem. Soc.* **2011**, *133*, 10062.
[11] T. Y. Chu, J. P. Lu, S. Beaupre, Y. G. Zhang, J. R. Pouliot, S. Wakim, J. Y. Zhou, M. Leclerc, Z. Li, J. F. Ding, Y. Tao, *J. Am. Chem. Soc.* **2011**, *133*, 4250.
[12] M. S. Su, C. Y. Kuo, M. C. Yuan, U. S. Jeng, C. J. Su, K. H. Wei, *Adv. Mater.* **2011**, *23*, 3315.
[13] L. Huo, S. Zhang, X. Guo, F. Xu, Y. Li, J. Hou, *Angew. Chem. Int. Ed.* **2011**, *50*, 9697.
[14] C. Y. Chang, C. E. Wu, S. Y. Chen, C. Cui, Y. J. Cheng, C. S. Hsu, Y. L. Wang, Y. Li, *Angew. Chem.Int. Ed.* **2011**, *50*, 9386.
[15] C. Y. Chang, Y. J. Cheng, S. H. Hung, J. S. Wu, W. S. Kao, C. H. Lee, C. S. Hsu, *Adv. Mater.* **2012**, *24*, 549.
[16] Y. Sun, C. J. Takacs, S. R. Cowan, J. H. Seo, X. Gong, A. Roy, A. J. Heeger, *Adv. Mater.* **2011**, *23*, 2226.
[17] T. Y. Chu, S. Alem, S. W. Tsang, S. C. Tse, S. Wakim, J. P. Lu, G. Dennler, D. Waller, R. Gaudiana, Y. Tao, *Appl. Phys. Lett.* **2011**, *98*, 253301.
[18] E. E. Havinga, W. Hoeve, H. Wynberg, *Synth. Met.* **1993**, *55*, 299.
[19] E. E. Havinga, W. Hoeve, H. Wynberg, *Polym. Bull.* **1992**, *29*, 119.
[20] P. M. Beaujuge, C. M. Amb, J. R. Reynolds, *Acc. Chem. Res.* **2010**, *43*, 1396.
[21] Y. Liang, L. Yu, *Acc. Chem. Res.* **2010**, *43*, 1227.
[22] C. H. Chen, C. H. Hsieh, M. Dubosc, Y. J. Cheng, C. S. Hsu, *Macromolecules* **2009**, *43*, 697.
[23] N. Kleinhenz, L. Yang, H. Zhou, S. C. Price, W. You, *Macromolecules* **2011**, *44*, 872.
[24] Y. Liang, D. Feng, Y. Wu, S. T. Tsai, G. Li, C. Ray, L. Yu, *J. Am. Chem. Soc.* **2009**, *131*, 7792.
[25] S. C. Rasmussen, R. L. Schwiderski, M. E. Mulholland, *Chem. Commun.* **2011**, *47*, 11394.
[26] J. P. Ferraris, A. Bravo, W. Kim, D. C. Hrncir, *J. Chem. Soc., Chem. Commun.* **1994**, *8*, 991.
[27] R. S. Ashraf, M. Shahid, E. Klemm, M. Al-Ibrahim, S. Sensfuss, *Macromol. Rapid Commun.* **2006**, *27*, 1454.
[28] H. Y. Chen, J. Hou, A. E. Hayden, H. Yang, K. Houk, Y. Yang, *Adv. Mater.* **2010**, *22*, 371.
[29] R. C. Coffin, J. Peet, J. Rogers, G. C. Bazan, *Nat. Chem.* **2009**, *1*, 657.
[30] E. J. Thomas, in *Science of Synthesis: Houben-Weyl Methods of Molecular Transformations*, Vol. *10* (Eds: T. L. Gilchrist, S. J. Higgins), Thieme, Stuttgart Germany **2000**,p. 185.
[31] J. Roncali, *Chem. Rev.* **1997**, *97*, 173.
[32] Y. Qin, J. Y. Kim, C. Frisbie, M. A. Hillmyer, *Macromolecules* **2008**, *41*, 5563.
[33] J. Y. Kim, Y. Qin, D. M. Stevens, V. Kalihari, M. A. Hillmyer, C. Frisbie, *J. Phys. Chem. C* **2009**, *113*, 21928.
[34] C. Quattrocchi, R. Lazzaroni, J. L. Bredas, R. Kiebooms, D. Vanderzande, J. Gelan, L. Van Meervelt, *J. Phys. Chem.* **1995**, *99*, 3932.
[35] R. Kisselev, M. Thelakkat, *Macromolecules* **2004**, *37*, 8951.
[36] D. L. Vangeneugden, D. J. M. Vanderzande, J. Salbeck, P. A. van Hal, R. A. J. Janssen, J. C. Hummelen, C. J. Brabec, S. E. Shaheen, N. S. Sariciftci, *J. Phys. Chem. B* **2001**, *105*, 11106.
[37] L. Goris, M. A. Loi, A. Cravino, H. Neugebauer, N. S. Sariciftci, I. Polec, L. Lutsen, E. Andries, J. Manca, L. De Schepper, D. Vanderzande, *Synth. Met.* **2003**, *138*, 249.
[38] D. Vangeneugden, R. Kiebooms, P. Adriaensens, D. Vanderzande, J. Gelan, J. Desmet, G. Huyberechts, *Acta Polym.* **1998**, *49*, 687.
[39] I. Polec, A. Henckens, L. Goris, M. Nicolas, M. A. Loi, P. J. Adriaensens, L. Lutsen, J. V. Manca, D. Vanderzande, N. S. Sariciftci, *J. Polym. Sci., Part A: Polym. Chem.* **2003**, *41*, 1034.
[40] T. Yamamoto, M. Usui, H. Ootsuka, T. Iijima, H. Fukumoto, Y. Sakai, S. Aramaki, H. M. Yamamoto, T. Yagi, H. Tajima, T. Okada, T. Fukuda, A. Emoto, H. Ushijima, M. Hasegawa, H. Ohtsu, *Macromol. Chem. Phys.* **2010**, *211*, 2138.

[41] S. E. Shaheen, D. Vangeneugden, R. Kiebooms, D. Vanderzande, T. Fromherz, F. Padinger, C. J. Brabec, N. S. Sariciftci, *Synth. Met.* **2001**, *121*, 1583.
[42] J. Hou, M. H. Park, S. Zhang, Y. Yao, L. M. Chen, J. H. Li, Y. Yang, *Macromolecules* **2008**, *41*, 6012.
[43] D. T. Hsu, C. H. Lin, *J. Org. Chem.* **2009**, *74*, 9180.
[44] L. T. Lin, H. Hart, *J. Org. Chem.* **1982**, *47*, 3570.
[45] R. Kisselev, M. Thelakkat, *Chem. Commun.* **2002**, *14*, 1530.
[46] Y. F. Li, Y. Cao, J. Gao, D. L. Wang, G. Yu, A. J. Heeger, *Synth. Met.* **1999**, *99*, 243.
[47] S. C. Price, A. C. Stuart, W. You, *Macromolecules* **2010**, *43*, 4609.
[48] L. Yang, H. Zhou, W. You, *J. Phys. Chem. C* **2010**, *114*, 16793.
[49] M. C. Yuan, M. Y. Chiu, S. P. Liu, C. M. Chen, K. H. Wei, *Macromolecules* **2010**, *43*, 6936.
[50] Y. Zhang, S. K. Hau, H. L. Yip, Y. Sun, O. Acton, A. K. Y. Jen, *Chem. Mater.* **2010**, *22*, 2696.
[51] P. T. Wu, F. S. Kim, R. D. Champion, S. A. Jenekhe, *Macromolecules* **2008**, *41*, 7021.
[52] Z. K. Chen, W. Huang, L. H. Wang, E. T. Kang, B. J. Chen, C. S. Lee, S. T. Lee, *Macromolecules* **2000**, *33*, 9015.
[53] Gaussian 09, Revision B.01, Gaussian, Inc., Wallingford CT, 2010, see supporting information for full citation.
[54] L. Chengteh, Y. Weitao, R. Parr, *Phys. Rev. B* **1988**, *37*, 785.
[55] A. Becke, *J. Chem. Phys.* **1993**, *98*, 5648.
[56] B. Carsten, J. M. Szarko, H. J. Son, W. Wang, L. Lu, F. He, B. S. Rolczynski, S. J. Lou, L. X. Chen, L. Yu, *J. Am. Chem. Soc.* **2011**, *133*, 20468.
[57] H. J. Son, B. Carsten, I. H. Jung, L. Yu, *Energy Environ. Sci.* **2012**, DOI: 10.1039/C2EE21608F
[58] V. D. Mihailetchi, L. J. A. Koster, P. W. M. Blom, C. Melzer, B. de Boer, J. K. J. van Duren, R. A. J. Janssen, *Adv. Funct. Mater.* **2005**, *15*, 795.
[59] Z. Chiguvare, V. Dyakonov, *Phys. Rev. B* **2004**, *70*, 235207.
[60] K. Vandewal, K. Tvingstedt, A. Gadisa, O. Inganas, J. V. Manca, *Nat. Mater.* **2009**, *8*, 904.
[61] M. D. Perez, C. Borek, S. R. Forrest, M. E. Thompson, *J. Am. Chem. Soc.* **2009**, *131*, 9281.
[62] R. J. Kline, M. D. McGehee, E. N. Kadnikova, J. Liu, J. M. Frechet, M. F. Toney, *Macromolecules* **2005**, *38*, 312.
[63] D. H. Kim, Y. D. Park, Y. S. Jang, H. C. Yang, Y. H. Kim, J. I. Han, D. G. Moon, S. J. Park, T. Y. Chang, C. W. Chang, M. K. Joo, C. Y. Ryu, K. W. Cho, *Adv. Funct. Mater.* **2005**, *15*, 77.
[64] Y. Liu, Y. Q. Liu, X. W. Zhan, *Macromol. Chem. Phys.* **2011**, *212*, 428.
[65] H. N. Tsao, D. Cho, J. W. Andreasen, A. Rouhanipour, D. W. Breiby, W. Pisula, K. Muellen, *Adv. Mater.* **2009**, *21*, 209.
[66] J. Liu, R. Zhang, G. Sauve, T. Kowalewski, R. D. McCullough, *J. Am. Chem. Soc.* **2008**, *130*, 13167.